

## Mathematical and numerical modelling of large creep deformations for annular rotating disks\*

K. SZUWALSKI, A. USTRZYCKA†

Faculty of Mechanical Engineering, Institute of Applied Mechanics,  
Cracow University of Technology, Cracow 31-864, Poland

**Abstract** A simulation model is presented for the creep process of the rotating disks under the radial pressure in the presence of body forces. The finite strain theory is applied. The material is described by the Norton-Bailey law generalized for true stresses and logarithmic strains. A mathematical model is formulated in the form of a set of four partial differential equations with respect to the radial coordinate and time. Necessary initial and boundary conditions are also given. To make the model complete, a numerical procedure is proposed. The given example shows the effectiveness of this procedure. The results show that the classical finite element method cannot be used here because both the geometry and the loading (body forces) change with the time in the creep process, and the finite elements need to be redefined at each time step.

**Key words** creep process, rotating disk, finite strain theory, simulation model

**Chinese Library Classification** O344

**2010 Mathematics Subject Classification** 65H10, 90C30, 76A99

### 1 Introduction

The concept of the mathematical description of large creep deformation for the full disk was formulated by Szuwalski for the first time<sup>[1]</sup>. The complexity of such problems is connected with both physical and geometrical nonlinearities and the existence of the additional time factor.

Szuwalski and Ustrzycka<sup>[2]</sup> introduced such modelling for rotating bars, and used it in the optimal design with respect to the ductile rupture time. The problems of the optimal design for the disks with respect to the brittle creep rupture were investigated in Refs. [3]–[5]. If the problem at issue is treated according to the results of the small strain theory (the rigidification theorem), then the cross section of the disk after deformations will be smaller than the calculated, which may lead to damage.

In this paper, the analysis is carried out for a thin (assumption of the plane stress state) annular disk with the internal radius  $A$  and the external radius  $B$ . The initial profile of the disk is described by the given function  $H(R)$ .

The disk, clamped on a rigid shift, rotates with the constant angular velocity, and is subjected to the body forces due to the resulting centrifugal forces. The additional external loading is a result of the centrifugal force, acting on the mass  $M$  uniformly distributed at the outer edge of the disk. Both the loadings change with the deformations of the disk, depending on the spatial coordinate. For the complex stress state, the law of the similarity stress and strain

---

\* Received Nov. 13, 2014 / Revised May 22, 2015

† Corresponding author, E-mail: anetaustrzycka@mech.pk.edu.pl

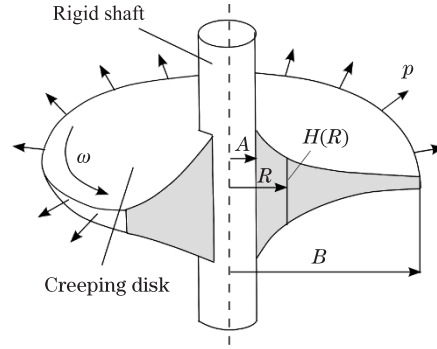


**Fig. 1** Model of annular rotating disk

deviators under the assumption of incompressibility is applied. Due to the necessity of the finite strain theory, this law is generalized for the true stresses and logarithmic strains. The Huber-Mises-Hencky concept of the effective stress is used.

Finally, the numeric approach to the mathematical model, consisting of four partial differential equations, is proposed. The algorithm for the numerical solution is presented, and some results for the chosen disk are shown. The present model may be used for the optimization of the metal disk rotating at a high speed and working in the elevated temperature. Examples may be the served rotators of turbines in power plants, jet engines, gear boxes, toothed wheels, motion and inertia wheels, brake back plates, etc. Both automobile industry and ship or aircraft technologies can profit from the presented analysis in the submitted manuscript. This research domain looks promising for the future studies in view of the multi-scale modeling applied to the creep rupture mechanisms.

## 2 Mathematical model

The large creep deformation behavior of the disk described above is investigated. To this end, a direct generalization of the Norton-Bailey creep law for the one-dimensional case is presented based on the logarithmic strain and the effective stress and strain. Four differential equations with suitable initial and boundary conditions are derived to govern the deformation and stress quantities. An algorithm for the numerical solution to these equations is proposed, and some numerical examples are presented.

The condition of the internal equilibrium for the element of the already deformed disk takes the form as follows:

$$\frac{1}{hr'} \frac{\partial}{\partial R} (h\sigma_r) + \frac{\sigma_r - \sigma_\vartheta}{r} + \frac{\gamma}{g} \omega^2 r = 0, \quad (1)$$

where  $R$  is the material (Lagrangian) coordinate and it is an independent variable,  $r$  is the spatial coordinate and it is a measure of the deformation,  $r'$  is the derivative of the spatial coordinate with respect to the material one,  $\sigma_r$  is the radial true stress,  $\sigma_\vartheta$  is the circumferential true stress,  $h$  is the current thickness of the disk,  $\omega$  is the angular velocity (constant in time),  $\gamma$  is the specific weight of the material, and  $g$  is the gravitational acceleration.

The physical law is adopted in the form of the nonlinear Norton creep law, which generalized for the complex stress state with the help of the Huber-Mises-Hencky hypothesis, i.e.,

$$\dot{\epsilon}_e = k\sigma_e^n, \quad (2)$$

where  $\sigma_e$  stands for the effective stress, and  $\dot{\epsilon}_e$  stands for velocity of the effective strain. The parameters  $k$  and  $n$  are the material constants in the experimentally designated Norton law.

Their values strongly depend on the temperature, and may be found in tables for several temperature ranges. The exponent  $n$  is usually rather larger (strong nonlinearity), and may exceed 10.

In our case, the finite strain theory is used. In the following equation, we have the true stresses and velocity of the logarithmic strains, i.e.,

$$\varepsilon_r = \ln \frac{\partial r}{\partial R} = \ln r', \quad \varepsilon_\vartheta = \ln \frac{r}{R}, \quad \varepsilon_z = \ln \frac{h}{H}. \quad (3)$$

Throughout, the partial derivatives with respect to the time  $t$  and the material coordinate  $R$  are designated by a superimposed dot and a prime, respectively.

The incompressibility of the material is assumed as follows:

$$HRdR = hrdr. \quad (4)$$

It is assumed that the creep behavior may be represented by a proportional relation between the logarithmic strain rate and the deviatoric stress, i.e.,

$$\begin{cases} \dot{\varepsilon}_r = \frac{3}{2}k\sigma_e^{n-1}(\sigma_r - \sigma_m), \\ \dot{\varepsilon}_\vartheta = \frac{3}{2}k\sigma_e^{n-1}(\sigma_\vartheta - \sigma_m), \\ \dot{\varepsilon}_z = \frac{3}{2}k\sigma_e^{n-1}(\sigma_z - \sigma_m), \end{cases} \quad (5)$$

where  $\sigma_m$  stands for the mean stress. Then, the second equation may be rewritten as follows:

$$\frac{\dot{r}}{r} = \frac{1}{2}k\sigma_e^{n-1}(2\sigma_\vartheta - \sigma_r). \quad (6)$$

Moreover, from (3)–(4), the following relation may be derived:

$$\varepsilon_r = \varepsilon_\vartheta + \ln \left( 1 + R \frac{\partial \varepsilon_\vartheta}{\partial R} \right). \quad (7)$$

By taking the time derivative and making use of (6), (7) may be converted to a form in the true stresses, i.e.,

$$\begin{aligned} & \sigma_r'((n-1)(2\sigma_r - \sigma_\vartheta)(2\sigma_\vartheta - \sigma_r) - 2\sigma_e^2) \\ & + \sigma_\vartheta'((n-1)(2\sigma_\vartheta - \sigma_r)^2 + 4\sigma_e^4) = 6\sigma_e^2 \frac{r'}{r} (\sigma_r - \sigma_\vartheta). \end{aligned} \quad (8)$$

Finally, the mathematical model, for large creep deformations of the annular disk, consists of four equations, i.e.,

$$\begin{cases} \frac{1}{hr'} \frac{\partial}{\partial R} (h\sigma_r) + \frac{\sigma_r - \sigma_\vartheta}{r} + \frac{\gamma}{g} \omega^2 r = 0, \\ \sigma_\vartheta' = \frac{6\sigma_e^2(\sigma_r - \sigma_\vartheta) \frac{r'}{r} - \sigma_r'((n-1)(2\sigma_r + \sigma_\vartheta)(2\sigma_\vartheta + \sigma_r) - 2\sigma_e^2)}{(n-1)(2\sigma_\vartheta - \sigma_r)^2 + 4\sigma_e^2}, \\ \frac{\dot{r}}{r} = \frac{r}{2}k\sigma_e^{n-1}(2\sigma_\vartheta - \sigma_r), \\ HRdR = hrdr. \end{cases} \quad (9)$$

This set contains four unknown, i.e., the true stresses-radial  $\sigma_r$ , the circumferential  $\sigma_\vartheta$ , the spatial coordinate  $r$  used for the description of deformations, and the current thickness of the disk  $h$ . Since three of these equations are differential, the initial and boundary conditions must be defined. At the beginning of the process, for  $t = 0$ , the spatial and material coordinates are the same. Therefore, the initial conditions take the form as follows:

$$r(R, 0) = R, \quad h(R, 0) = H(R). \quad (10)$$

The boundary conditions at the inner radius  $A$  depend on the way, in which the disk is connected with the rigid shaft. In case of the welded joint, neither the thickness nor the spatial coordinate can change there, i.e.,

$$h(A, t) = H(A), \quad r(A, t) = A. \quad (11)$$

The second condition leads to the relationship between the true stresses, i.e.,

$$\sigma_r(A, t) = 2\sigma_\vartheta(A, t). \quad (12)$$

At the outer radius  $B$ , the external loading results from the centrifugal force acting on the uniformly distributed mass  $M$  under the assumption that this mass will remain to be uniformly distributed during the deformation process.

Then, the radial stress at the external radius can be given by

$$\sigma_r(B, t) = p = \frac{M\omega^2}{2\pi h(B)}. \quad (13)$$

### 3 Dimensionless quantities

With the initial and boundary conditions (10)–(13), the four equations given by (9) may be solved only by means of the numerical procedures. To this aim, the dimensionless quantities, further denoted by the overbars, must be introduced. The material and spatial coordinates are referred to the initial external radius of the disk as follows:

$$\bar{R} = \frac{R}{B}, \quad \bar{r} = \frac{r}{B}. \quad (14)$$

The initial and current thicknesses of the disk are related to the mean thickness of the full disk of the given volume  $V$  and the radius  $B$ , i.e.,

$$\bar{H} = \frac{\pi \cdot B^2}{V} H, \quad \bar{h} = \frac{\pi \cdot B^2}{V} h. \quad (15)$$

The dimensionless true stresses are obtained by dividing the following quantity:

$$s = \frac{M\omega^2}{2\pi h_m} = \frac{M\omega^2 B^2}{2V}. \quad (16)$$

Thus,

$$\bar{\sigma}_i = \frac{2V}{M\omega^2 B^2} \cdot \sigma_i, \quad i = r, \vartheta. \quad (17)$$

Also, the dimensionless time can be introduced as follows:

$$\bar{t} = \frac{t}{\tau}, \quad (18)$$

where  $\tau$  denotes the time of the ductile rupture for a full plane disk subject to the uniform radial tension  $p$  given by (13) at the outer edge. For such a disk, the stresses are given by

$$\sigma_e = \sigma_r = \sigma_\theta = p. \quad (19)$$

Then, the third equation in (9) produces

$$\frac{1}{h} \frac{dh}{dt} = -k \left( \frac{M\omega^2}{2\pi h} \right)^n. \quad (20)$$

From this equation, the time to the rupture  $\tau$ , at which the thickness of the disk becomes vanishing, may be derived as follows:

$$\tau = \frac{1}{nk \left( \frac{M\omega^2}{2\pi h_m} \right)^n} = \frac{1}{nks^n}. \quad (21)$$

The dimensionless time is finally defined by

$$\bar{t} = \frac{t}{\tau} = nks^n t. \quad (22)$$

By applying all the dimensionless quantities introduced above, our set of the four equations can be rewritten as follows:

$$\begin{cases} \bar{\sigma}'_r = \frac{\bar{r}'}{\bar{r}} (\bar{\sigma}_r - \bar{\sigma}_\theta) - 2 \cdot \bar{r} \bar{r}' \mu - \frac{\bar{h}'}{\bar{h}} \bar{\sigma}_r, \\ \bar{\sigma}'_\theta = \frac{6\bar{\sigma}_e^2 (\bar{\sigma}_r - \bar{\sigma}_\theta) \frac{\bar{r}'}{\bar{r}} - \bar{\sigma}'_r ((n-1)(5\bar{\sigma}_r \bar{\sigma}_\theta - 2\bar{\sigma}_r^2 - 2\bar{\sigma}_\theta^2) - 2\bar{\sigma}_e^2)}{(n-1)(2\bar{\sigma}_\theta - \bar{\sigma}_r)^2 + 4\bar{\sigma}_e^2}, \\ \frac{d\bar{r}}{d\bar{t}} = \frac{\bar{r}}{2n} (\bar{\sigma}_r^2 + \bar{\sigma}_\theta^2 - \bar{\sigma}_r \bar{\sigma}_\theta)^{\frac{n-1}{2}} (2\bar{\sigma}_\theta - \bar{\sigma}_r), \\ \bar{h} = \frac{\bar{H} \bar{R}}{\bar{r}' \bar{r}}. \end{cases} \quad (23)$$

In those equations, the following auxiliary quantities are used:

$$\mu = \frac{\gamma V}{gM}, \quad \beta = \frac{A}{B}, \quad (24)$$

where  $\mu$  is the ratio of the disk mass to the mass distributing at the outer radius, while  $\beta$  is the ratio of the internal to the external radius. The non-dimensionalized equations given by (22) are convenient for numerical treatments.

The four equations given in (22) may be numerically integrated with the initial conditions (11). Here, they are presented in the dimensionless form as follows:

$$\bar{r}(\bar{R}, 0) = \bar{R}, \quad \bar{h}(\bar{R}, 0) = \bar{H}(\bar{R}). \quad (25)$$

The boundary conditions (12) take the form as follows:

$$\bar{h}(\beta, \bar{t}) = H(\beta, 0), \quad \dot{\bar{r}}(\beta, \bar{t}) = 0, \quad (26)$$

resulting in that

$$\bar{\sigma}_r(\beta, t) = 2\bar{\sigma}_\theta(\beta, t). \quad (27)$$

The condition at the external radius, where the mass  $M$  is distributed, takes the form as follows:

$$\bar{\sigma}_r(1, t) = \frac{1}{\bar{h}(1, t)}. \quad (28)$$

4 Numerical model

The algorithm of the simulation model of the creeping process for an annular disk is made in MAPLE to obtain the symbolic results<sup>[6]</sup>. In the present algorithm, the physical properties of the material are introduced by the exponent  $n$  in Norton's law (2), varying the width of the disk by the parameter  $\beta$  in (24). The parameter  $\mu$  in (24) gives the possibility to change the load applied at the outer edge of a disk.

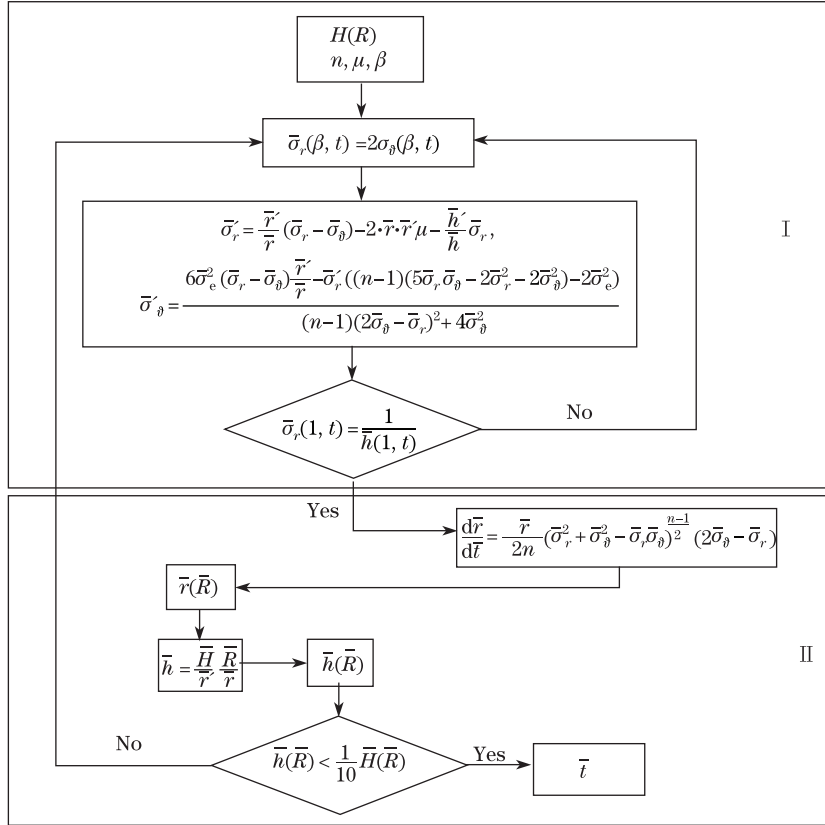


Fig. 2 Algorithm of numerical calculation flow chart

The structure of the algorithm is shown in Fig.2. For the sake of clarity, two parts are introduced and explained.

In the first part (I), the stress distribution for the given geometry of the disk is found. It requires integration of the two first equations in (23) with respect to the material coordinate with the initial conditions in (25). The width of the disk is divided into fifty parts initially of equal length. The program assigns a procedure by use of the Runge-Kutta method of the fourth-order. The values of the stresses at the radius  $A$  must be assumed in such a way that the result of the integration satisfies at the outer radius boundary condition (26) with the given accuracy. To this aim, the recurrential procedure must be applied because the initial values of the stresses for the inner radius  $A$  are unknown.

In the second part (II), i.e., the integration with respect to time, for the already known distribution of the stresses (established in part I), the geometry changes of the disk are calculated. The third equation of (23) is integrated with respect to time by use of Euler's method. The time step varies. At the beginning, the time step may be a little large (the geometry changes slowly). For the time close to the time to rupture, the time step must be small, as the creep

process significantly accelerates. This is realized by the demand of the constant elongation of the last part of the disk at the velocity of the spatial radius calculated from the third equation in (23). After new spatial coordinates are found, the current thickness  $h$  at these points is calculated from the only algebraical equation, i.e., the incompressibility condition (the fourth equation in (23)). With the parameters for the deformed disk found in this way, the stress distribution may be calculated, repeating the procedure in Part I. All the time steps are summarized, giving the total time of the work for the given disk. The calculation may be carried out until the condition of the ductile rupture is satisfied. Here, this condition is approximated by the thickness reduction to the tenth of the initial thickness.

## 5 Numerical results

As an example, the creep process for a disk with the initial geometry given by  $\overline{H}(\overline{R}) = 4.7 - 10\overline{R} + 6.1\overline{R}^2$  is shown in Fig. 3.

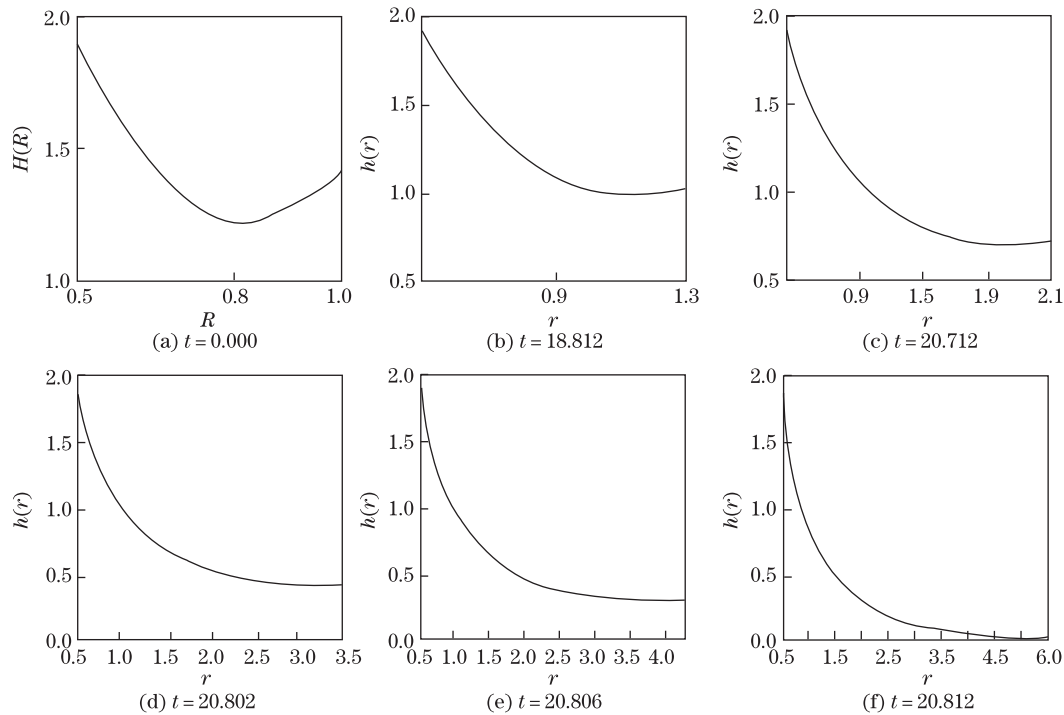


**Fig. 3** Process of creep for annular rotating disk

For the time  $t = 18.812$ , the shape of the disk is almost the same as the initial profile of the disk, while the ductile rupture reaches when  $t = 20.812$ .

The creep process of the disk significantly accelerates in its final phase. The change of the external radius  $\overline{b}(t)$  in the time is shown in Fig. 4. At the moment of rupture, the external radius of the disk increases six times. The qualitative results, i.e., the history of the creep process, prove the reliability of the procedure. The majority of the life-time strains (displacements) are rather small, but permanently grow when the body forces enlarge. Finally, the creep process rapidly accelerates, leading to the ductile rupture.

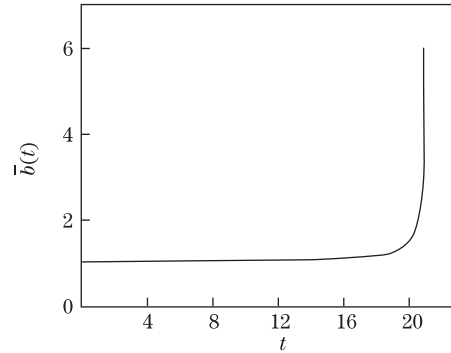


**Fig. 4** Change of external radius  $\bar{b}(t)$  in time

The procedure described above may be applied to the optimal design problem with respect to the ductile creep rupture time. Some general remarks on the optimization in the creep condition were formulated by Żczkowski<sup>[7]</sup>. The results for the annular disks may be found in Refs. [2] and [8].

## 6 Conclusions

In engineering practice, many rotating disk problems with possible large creep deformations may be encountered, e.g., turbines of engines and power plants. The problem is even more complicated, as the loadings resulting from the rotation of the disk (centrifugal forces) depend on the spatial coordinate and the change in time. The set of four differential equations describing the problem is derived, and the numerical procedure for solving these equations is proposed by use of the finite strain theory. The example shows that, deformations may be very large, and the process accelerates significantly at its end.

## References

- [1] Szuwalski, K. Optimal design of disks with respect to ductile creep rupture time. *Structural Optimization*, **10**, 54–60 (1995)
- [2] Szuwalski, K. and Ustrzycka, A. Optimal design of bars under nonuniform tension with respect to mixed creep rupture time. *International Journal of Non-Linear Mechanics*, **47**, 55–60 (2012)
- [3] Farshi, B. and Bidabadi, J. Optimum design of inhomogeneous rotating disks under secondary creep. *International Journal of Pressure Vessels and Piping*, **85**, 507–515 (2008)
- [4] Jahed, H., Farshi, B., and Bidabadi, J. Minimum weight design of inhomogeneous rotating discs. *International Journal of Pressure Vessels and Piping*, **82**, 35–41 (2005)
- [5] Singh, S. B. One parameter model for creep in a whisker reinforced anisotropic rotating disc of Al-SiC composite. *European Journal of Mechanics, A: Solids*, **27**, 680–690 (2008)
- [6] Waterloo Maple Incorporated. *Advanced Programming Guide*, Springer-Verlag, New York (2010)
- [7] Żczkowski, M. Optimal structural design under creep conditions. *Applied Mechanics Reviews*, **12**, 453–461 (1988)
- [8] Szuwalski, K. and Ustrzycka, A. The influence of boundary conditions on optimal shape of annular disk with respect to ductile creep rupture time. *European Journal of Mechanics, A: Solids*, **37**, 79–85 (2012)